63-014A

AIAA ELECTRIC PROPULSION CONFERENCE
BROADMOOR HOTEL, COLORADO SPRINGS, COLO. MARCH 11-13, 1963

DIAGNOSTIC STUDIES OF A PINCH PLASMA ACCELERATOR

by
Donald P. Duclos,
Leonard Aronowitz,
Frederic P. Fessenden and
Peter B. Carstensen

Republic Aviation Corporation
Farmingdale, L.I., New York

63014 A

DIAGNOSTIC STUDIES OF A PINCH PLASMA ACCELERATOR [1]

by

Donald P. Duclos[2], Leonard Aronowitz[2],
Frederic P. Fessenden[3] and Peter B. Carstensen[4]

Republic Aviation Corporation, Farmingdale, N.Y.

ABSTRACT

Characteristics of a pinch plasma accelerator were investigated by means of measurements of the total discharge current, capacitor voltage, magnetic field distribution and light front velocity. The current distribution and J x B force on the plasma were calculated. The results show that a current sheet resulting from the first half-cycle of current propagates along the electrodes, becoming more diffuse with time. It was observed that there are regions in the sheet where the direction of current density shows local reversals. Magnetic probes indicate that the motion of the current sheet turns from an initially radial to an axial direction and that the magnetic force on the current sheet is essentially in the direction of plasma motion. The impulse produced by J x B forces in the accelerator was computed and was found to be about 80% of the measured thrust. All of the net energy output of the capacitor bank was transferred to the accelerator in the first 2.4 μsec.

---

1. This work was supported in part by AFOSR under Contract AF 49 (638)-552.

2. Specialist Scientific Research Engineer, Power Conversion Systems Div.

3. Senior Scientific Research Engineer, Power Conversion Systems Div.

4. Scientific Research Engineer, Power Conversion Systems Div.

INTRODUCTION

This paper reports results of a continuing program for investigating the characteristics of a pinch plasma accelerator. Initial measurements were reported at the 1962 ARS Electric Propulsion Conference (1)[5].

The accelerator is shown schematically in Fig. 1. The pinch discharge takes place between a pair of nozzle-shaped aluminum electrodes of approximately quarter circle cross section. The maximum internal diameter of the electrodes is eight inches. In order that probes could be inserted between the electrodes, holes were drilled through the outer electrode at positions 1 through 4 shown in Fig. 2. The distances shown between probes were measured along the centerline of the gap between the electrodes. Unless otherwise noted, the accelerator utilized a capacitor bank of twelve 10-μf capacitors, arranged symmetrically about the electrodes, which were charged to a potential of 3 kv giving an energy per discharge of 540 joules. The discharge is initiated by briefly opening a solenoid valve which admits a pulse of gas into the interelectrode space through a set of orifices. The orifices are located in the inner electrode between positions 1 and 2. The gas used was nitrogen unless otherwise specified. The accelerator was operated in a vacuum chamber held at a pressure of less than 5×10^{-4} mm Hg.

---

5. Numbers in parentheses indicate References at end of paper.

Fig. 3 shows the voltage measured at the capacitor terminals V_c and the total discharge current I. The voltage was measured with a Tektronix Type P6013 voltage divider and the total current with a Rogowski coil and a simple RC integrating circuit. It is seen that the greatest portion of the voltage drop occurs during the first microsecond. The half-cycle period of the current is slightly over 3 μsec.

Idealized theory of a linear pinch (e.g., see Ref. 2) indicates that the discharge current will begin to flow at the outer periphery of the electrodes. The current produces an azimuthal magnetic field which rises from zero at the leading edge of the current sheet to its maximum value at the trailing edge. The resulting magnetic pressure accelerates the current sheet in the radial direction. As the current sheet moves inward, the magnetic force produced acts like a magnetic "piston" and picks up and ionizes the neutral gas ahead of it. For purposes of calculation, the current sheet is usually assumed to be infinitely thin and the plasma in the sheet to have an infinite electrical conductivity. Also, the magnetic piston is sometimes assumed to pick up and accelerate all of the gas ahead of it (snowplow model) or to accelerate a fixed amount of gas (slug model). In the pinch plasma accelerator, the curved electrodes allow the plasma to turn in the axial direction and consequently it can be ejected from the accelerator.

One of the purposes of this study was to determine how closely the characteristics of the accelerator resemble the idealized model. In particular, it was desired to determine if the motion of the

current sheet turns from the radial to the axial direction and if the magnetic force or "piston" constitutes the primary means of accelerating the plasma, or if the plasma is accelerated by some other means.

MAGNETIC FIELD MEASUREMENTS

In order to study the characteristics of the current sheet, the magnetic field was measured by means of magnetic probes. The probes were constructed of Teflon-covered No. 28 magnet wire wound into an 8-turn solenoid approximately 3 mm in diameter and 3 mm long. The cable from the probe was terminated (3) to provide a flat frequency response up to 8 Mc. The probes were used with simple RC integrating circuits with a 47 μsec time constant. Differential preamplifiers were used to amplify the oscilloscope signal. Although the probes were in direct contact with the plasma, the Teflon coating provided a satisfactory operating life. It was found that the operating life of the probes could be extended by covering the Teflon coated wire with a thin coating of epoxy resin. Earlier attempts were made to construct a probe which would withstand the plasma environment by enclosing them with quartz covers about 7 mm in diameter and 8 mm long. However, the covers lowered the output signal appreciably and thus were abandoned.

Reproductions of typical oscilloscope traces of the azimuthal magnetic field B_θ at the four probe positions are shown in Fig. 4.

It is seen that the time of arrival of the magnetic field at a given position is later than at the previous position, indicating that the magnetic field does propagate down the electrodes.

When all of the discharge current is confined to a single current sheet, B_θ is zero ahead of the current sheet and, at a given position behind the sheet, is proportional to the total discharge current. The current flow during the second half-cycle is in the opposite direction to that in the first half-cycle, and thus B_θ behind the sheet is also in the opposite direction. Since the initiation of the discharge takes place near position 1, the probe signal at this position has an approximately damped sinusoidal form corresponding to the total discharge current. However, it is seen from Fig. 4 that at positions 2 through 4 the magnetic field always remains positive, or has at most a slight negative dip. This demonstrates that the current distribution resulting from the second half-cycle does not propagate down the electrodes but remains between the insulator and position 2. This phenomenon is similar to the "self-crowbarring" discussed by Gooding, Hayworth, and Lovberg(4). However, they observed a second breakdown which occurred before the second half-cycle of current.

Times of arrival were also measured at positions 1 through 4 with a photocell and a single electric probe grounded through a 5-ohm resistor(1). Comparison of the times of arrival showed that the

magnetic probe signal arrived first, followed by the electric probe signal followed by the photocell signal. The time of arrival of the magnetic probe signal was about 0.4 μsec earlier than the photocell signal. The electric probe signals were roughly midway between the magnetic probe and photocell signals, being somewhat closer to the photocell time of arrival. The delay of the photocell signal could possibly be explained in terms of the relaxation times involved for light emission. The delay of the electric probe signal is more difficult to explain. It indicates that there is some current diffusion ahead of the main body of the plasma being accelerated. However, the electric probes showed a small precursor signal preceding the magnetic probe signal which could at least partially account for this diffusion. The cause of the precursor is not known but it could be due to photo-ionization from the main current sheet.

It is seen from Fig. 4 that the oscilloscope traces sometimes show a small precursor magnetic field beginning at about $t = 0$. These precursors are undoubtably due to small asymmetries in the current distribution, possibly of the "spoke" type(4). The precursor can be positive or negative depending on the location of the spoke relative to the probe. The current distribution in the discharge, however, is essentially symmetric. This was shown in symmetry tests in which four magnetic probes were located at 90° intervals about the axis of symmetry of the electrodes at the same distance from the insulator. A set of four

probes was located at each of the four probe positions shown in Fig. 2. Comparison of the magnitude and time of arrival of the B_θ signal at each position indicated that the discharge was essentially symmetric above capacitor potentials of 2.5 kv. These results indicated that the discharge was a sheet which was nearly uniform in the azimuthal direction. Consequently, the "spoke" asymmetries which cause the precursor signal are small pertubations of the main sheet discharge and would not be expected to have a significant influence on the characteristics of the accelerator.

From the oscilloscope traces, the magnetic field can be plotted as a function of s at various times where s is the distance from the insulator measured along the centerline of the interelectrode gap. The data was taken at eight positions along the electrodes. (This was accomplished by constructing probes so that the magnetic field could be measured at two s points from each of the hole locations shown in Fig. 2.) Probes were also placed beyond the exit ($s = 17.0$ cm) to measure the trapped magnetic field in the plasma exhaust. The value of the magnetic field at the insulator ($s = 0$) was calculated from the total current, as measured by the Rogowski coil, from the relation

$$B_\theta = \frac{\mu_o I}{2 \pi r_o} \qquad [1]$$

where r_o is the inside radius of the insulator measured from the symmetry axis of the electrodes.

The results are shown in Fig. 5. The propagation of the magnetic field down the electrodes is apparent. If the thickness of the current sheet is taken as the distance over which the magnetic field rises from zero to its maximum value, the minimum thickness is about 4 cm at 1.0 μsec. This is in marked contrast to the infinitely thin current sheet assumed in theoretical calculations.

Since the leading edge of the current sheet advances faster than the peak, the current sheet becomes thicker as it moves toward the exit. This same general behavior was observed by Burkhardt and Lovberg(5) in a coaxial plasma gun. It is seen that a second peak appears at $s = 3$ cm at about the time the current sheet reaches the exit (3.5 μsec) and disappears about 1 μsec later. The reason for this second peak is not known.

Since the second half-cycle of current begins at about 3 μsec, B_θ at the insulator becomes negative at that time. The first probe (position 1 at $s = 1.1$ cm) does not record a negative magnetic field until about 4.0 μsec, indicating that the second current sheet remains near the insulator up to this time. For later times, the second current sheet is seen to have a slightly smaller thickness than the first current sheet, but does not propagate down the electrodes.

It is of interest to compare the behavior of the second current sheet with results of photocell measurements of the light fronts produced by the current sheets. The light fronts were recorded at positions

1 through 4 with RCA 1P42 photocells. The first, second, and third light fronts were recorded on the oscilloscope trace of the photocell output. It is possible that there were succeeding light fronts after the third, but if they did exist, they were not detected by the photocell, indicating that their light intensity was a small fraction of the intensity of the first front. Even the third light front was of very small amplitude, and it appeared to be rather diffuse. Consequently, its velocity could not be determined with any degree of accuracy.

Fig. 6 shows the velocities of the first and second light fronts as a function of the capacitor energy. It is seen that, as expected, the velocity of the first light front between positions 3 and 4 is greater than the velocity between 1 and 2. However, the velocity of the second light front decreases as it travels along the electrodes. It is noted that, between positions 1 and 2, the velocity of the second front is initially higher than that of the first front. This may be due to the fact that the second discharge takes place in a gas which is already partially ionized.

The deceleration of the second front agrees well with the magnetic probe data. (Note that the second light front reaches position 3, $s = 11.6$ cm, between 6 and 7 μsec and position 4, $s = 15.1$ cm, between 7 and 8 μsec.) The magnetic field due to the second half-cycle does not propagate beyond position 2 ($s = 6.2$ cm). Concurrently, there is still a residual magnetic field due to the first half-cycle beyond

this point. Consequently, instead of being driven by a magnetic field, as in the case for the plasma associated with the first light front, the plasma associated with the second front propagates through a magnetic field. This together with the viscous drag which exists, accounts for its deceleration. Therefore, it can be concluded that the accelerator produces only one pinch which accelerates the plasma associated with the first light front and which is due to the first half-cycle of current.

CURRENT SHEET ORIENTATION

In order to determine if the current sheet remains perpendicular to the electrodes while its motion changes from the radial to the axial direction, the time of arrival of the magnetic field was measured transverse to the plasma flow for both positive and negative polarity of the inner electrode. (The accelerator is normally operated with the center electrode positive.) The measurements were made by mounting three magnetic probes perpendicular to the electrodes at each position. Preliminary results showed that for both polarities the current sheet position at the inner electrode and the position at the outer electrode differed by less than about 1 cm along the entire electrode length so that the current sheet remained roughly perpendicular to the electrodes at all times. More precise measurements are in progress to determine the exact shape and cant of the current sheet.

It has been suggested by Gloersen(6) that in a pinch accelerator "the initial radial motion of the plasma is converted to axial motion solely by collisions with the curved electrode surfaces, since no appropriately curved magnetic field lines are present for this purpose." However, the small cant and perpendicular orientation of the current sheet indicates that the magnetic force is acting on the plasma approximately in the direction of plasma motion, i.e., in the direction of s, and throughout the entire length of the electrodes. Gloersen's statement implies that the plasma being accelerated must collide with the inner electrode before it changes direction. However, since the plasma being accelerated is in the current sheet and subject to magnetic forces, it can change direction without collisions with the inner electrode. Undoubtedly, some of the plasma does collide with the walls and these collisions do affect the orientation of the current sheet, but the fraction of the plasma making these collisions should be small.

There are two physical reasons why the motion of the current sheet changes from the radial direction. The first is that, at least ahead of the current sheet, the electric field applied to the electrodes from the capacitors will be perpendicular to the electrodes. The current will tend to follow the direction of the electric field. The second reason is that, once the current sheet has begun to turn, the magnetic pressure, which varies as r^{-2}, is greater at the inner electrode and thus will tend to turn the current sheet more. This problem is currently being investigated analytically(7).

CURRENT DISTRIBUTION

From the B_θ vs s curves, a current distribution function can be calculated. This function j(s) is defined by $dI = j(s)ds$ where dI is the current crossing the element of area generated by rotating ds about the axis of symmetry of the electrodes. (Note that j(s) has the dimensions of current per unit length.) The current is assumed to be uniformly distributed about the axis of symmetry of the electrodes. Therefore the value of B_θ at position s is given by

$$B_\theta = \frac{\mu_o I_s}{2 \pi r_s} \qquad [2]$$

where I_s is the current in amperes between s and the end of the current distribution which is at a position s_1, $\mu_o = 4\pi \times 10^{-7}$ h/m, and r_s is the distance from s in meters to the symmetry axis. Since

$$I_s = \int_s^{s_1} j(s)ds \qquad [3]$$

substituting Eq. 3 into Eq. 2 and differentiating with respect to s yields the expression for j(s). Thus

$$j(s) = -\frac{2\pi}{\mu_o} \frac{\partial}{\partial s} (r_s B_\theta) \qquad [4]$$

The current density J(s) is related to j(s) by $J(s) = j(s)/2\pi r_s$.

Various schemes were used for computing j(s) from the measured values of B_θ. Hand computation appeared to be the most reliable method. The most difficult and time consuming part of the hand computation, as well as the operation in which the most uncertainty was introduced, was the determination of the derivative of the $r_s B_\theta$ curve which was obtained by fitting slopes by eye to the curve. Consequently, digital computer programs were used to simplify data processing. The most successful computer method used parabolic interpolation between data points to obtain the derivative. However, this procedure introduced a few doubtful peaks into the computed results. Another scheme used a higher order polynomial least squares fit to the data points.

As a check on the accuracy of the j(s) distributions, the integral

$$I = \int_0^{s_1} j(s)ds \qquad [5]$$

was compared with the discharge current measured with a Rogowski coil. Both of these digital computer methods gave fair agreement with the current values measured by the Rogowski coil but the agreement of the hand computed results was better. The comparison of the hand computed results and the Rogowski coil measurement is shown in Fig. 7 and the agreement is seen to be very good up to the peak of the second half-cycle.

Plots of j(s) vs. s at 0.5 μsec intervals are shown in Fig. 8. It is seen that the current sheet is concentrated near $s = 0$ at the beginning of the discharge. During this interval, current densities in excess of 2×10^7 amp/m^2 occur. After 1 μsec the current sheet moves down the electrodes becoming progressively more diffuse. Similar results were obtained using nine 40μf capacitors charged to 1.44 kv which were substituted for the capacitor bank used in the study.

The reversal of current direction at small values of s occurring during the first half-cycle of the total discharge current can be seen in Fig. 8. This reversal of current is due to loop currents which have been observed in other plasma accelerators using capacitive discharges (8). During the second quarter-cycle, the total discharge current is decreasing which tends to decrease the magnetic flux in the interelectrode space. Because this space is filled with plasma, a relatively good conductor, eddy currents are induced to oppose the change in flux. This current takes the form of closed loops in the plasma. Near the leading edge of the current distribution the loop currents are in the same direction as the current from the capacitor bank while at the rear of the distribution the loop currents are in the opposite direction. It should be noted, however, that this explanation does not account for the loop currents during the first quarter-cycle (before 1.5 μsec).

An interesting phenomenon was observed in the current distributions for times greater than 3.0 μsec. It is noted in Fig. 8 that at 3.0 μsec, two positive peaks separated by a negative region appear. These peaks correspond to the two peaks noted in the B_θ vs s curves. Apparently the direction of current density at any instant may show regions in which there are local reversals in current direction. The reversal of current near the insulator caused by eddy currents during the second quarter-cycle has already been mentioned. Because of the decreasing values of B_θ and the broadening of the B_θ distribution, the sensitivity of the measurements becomes insufficient to accurately resolve the local structure at substantially later times. Investigations will be made to ascertain the cause and importance of this structure in the current distribution since it will influence the J x B force distribution and may play a role in determining the details of accelerator characteristics.

J x B FORCE DISTRIBUTION AND IMPULSE

The magnetic (J x B) force distribution acting on the plasma can be calculated from the magnetic field and current distributions and is plotted in Fig. 9 at 0.5 μsec intervals. A force distribution function f(s) is defined by the expression $dF = f(s)ds$ where dF is the magnetic force on an element of plasma contained between two planes located at

s and s + ds, the planes being taken normal to s. The distribution f(s) is given by

$$f(s) = j(s)\, B_\theta(s)\, h(s) \qquad [6]$$

where h is the interelectrode gap spacing. The total force F(t) on the plasma at time t is the integral of f(s) over the length of the electrodes. More accurately, it is the integral over the current distribution, some of which extends outside the nozzle at later times. However, the contribution of this external portion is small.

The impulse given to the plasma by the J x B force is the integral of F(t) over the time of the discharge. Characteristics of the accelerator will depend on the details of the processes by which momentum is transferred to the mass of the plasma. However, the impulse imparted to the plasma which is determined from the distributions of J and B is independent of momentum transfer mechanisms.

When comparing the impulse imparted to the plasma by F(t) with the impulse of the accelerator as measured on a thrust stand, some uncertainty is introduced by the negative portions of the f(s) curves which may be quite large at small values of s (see Fig. 9). These forces, which are directed away from the exit, will accelerate plasma toward the insulator. This plasma flow will most likely move toward the insulator and be stagnated there. Then by re-expanding, it could contribute some positive impulse to the accelerator. However,

such a conversion from J x B to thermal impulse would be relatively inefficient. Therefore the negative portions of f(s) were neglected and only the positive leading portions were used to compute F(t). For example, from the J x B curve for 3.0 μsec in Fig. 9, it can be seen that f(s) is positive for s greater than approximately 8 cm. Only this positive portion of the f(s) distribution was used to calculate F(t) at 3.0 μsec. The values of f(s) for s less than 8 cm where f(s) has both negative and positive regions was neglected. This method of calculating F(t) neglects the possibility that some of the mass acted upon by a positive force could subsequently be acted upon by a negative force. Consequently, some of the impulse would be lost. Unfortunately, it is exceedingly difficult to estimate what fraction of the mass would be affected. Certainly the negative force near the insulator at later times does not affect the plasma being accelerated by the first half-cycle and thus can safely be neglected.

A plot of the relative value of F(t) vs t is shown in Fig. 10. The impulse calculated from this plot is approximately 80% of the impulse produced by the accelerator as measured by a thrust stand. If both the positive and negative portions of the f(s) curve are used to compute F(t), the calculated impulse is about 50% of the measured value. However, as previously mentioned, this value is certainly low.

These results are consistent with the previously mentioned probe measurements which showed that the magnetic force is essentially in

the direction of plasma motion indicating that it could be the principal force acting on the plasma. The agreement between computed and measured impulse indicates that the impulse comes primarily from the J x B force and that other contributions to the impulse such as the subsequent hot gas flow are small. It also indicated that viscous loss mechanisms in the electrodes which could prevent the full J x B impulse from appearing as accelerator impulse are small.

CAPACITOR POWER AND ENERGY OUTPUT

From simultaneous capacitor voltage and total discharge current measurements, as illustrated in Fig. 3, the power output of the capacitors was calculated as a function of time. The result is shown in Fig. 11 for a capacitor potential of 3 kv. The negative portions of the curve represent the power returned to the capacitors from the inductive elements of the circuit. It is seen that after 2.4 μsec the power output of the capacitors is essentially balanced by the power returned. This is shown more clearly by the curve representing the total energy transferred from the capacitors to the accelerator as a function of time which was obtained by integrating the power curve. At 2.4 μsec, the energy output of the capacitors is 260 joules. Although the energy output reaches a maximum of 270 joules at several later times, the total energy output after the current rings out at about 20 μsec is only 255 joules.

The power and energy output are in qualitative agreement with the velocity and acceleration of the current sheet as determined by the magnetic probe and photocell data. It was found that the current sheet accelerates up to about 2 μsec. The current sheet subsequently travels at constant velocity until it reaches the exit. The current sheet appears to stop accelerating because the net power input to the accelerator is approaching zero. The probable reason that the magnetic field due to the second half-cycle does not propagate down the electrodes is that there is no net power input during the second half-cycle.

McIlroy(9) has shown in a dimensionless snowplow analysis that for optimum performance the plasma should reach the accelerator exit when the voltage reaches zero. The obvious physical reason for this result is that after the voltage goes through zero, the power input to the accelerator becomes negative, as illustrated by Fig. 11. It can be concluded that the performance of this accelerator could be improved by redesigning the electrodes so that the current sheet reached the exit at 2.4 μsec. An average value of the sheet position would have to be used, however, since the thickness of the current sheet is relatively large at this time.

It is noted that the 255 joules transferred from the capacitors to the accelerator is less than half of the 540 joules stored in the capacitor bank at 3 kv. The remaining energy must be dissipated in the

capacitors as an I^2R loss. The capacitors are therefore not well suited to efficient operation with this type of accelerator.

The efficiency of a plasma accelerator obviously also depends on the fraction of the energy leaving the capacitors which is converted to plasma kinetic energy. The efficiency of this accelerator is low because there is a poor "match" between the various electrical, geometric, and magnetogasdynamic parameters. This low efficiency can be advantageous in diagnostic studies by making the discharge current less sensitive to changes in some of the parameters. Thus the effects of varying these quantities can be studied while holding the discharge current relatively constant.

The dependence of the discharge current on the magnetogasdynamic characteristics can be seen in Fig. 12 which shows the discharge current for a type of accelerator similar to the one discussed in this paper, except that the parameters are better matched. Fig. 12a shows the trace which results from discharging the capacitor bank by connecting a short circuit across the exit end of the electrodes. The trace is seen to be a typical damped LC discharge. Fig. 12b shows the discharge current occurring during actual plasma acceleration. It is seen that the current is highly damped, the second quarter-cycle being almost negligible. Therefore, a greater percentage of the input energy should be transferred to the plasma.

EFFECT OF PROPELLANT

The plasma exhaust velocity of the accelerator was determined using four gases as the propellant: hydrogen, helium, nitrogen, and freon. The exhaust velocity was determined as a function of the energy stored in the capacitors from time of arrival data obtained at positions 5 and 6 by means of photocells. (See Fig. 2.) The gas supply pressure was set just slightly higher than the minimum value which would cause breakdown. The approximate supply pressures were: hydrogen - 40 mm Hg, helium - 60 mm Hg, nitrogen - 40 mm Hg, and freon - 10 mm Hg.

The results are presented in Fig. 13. It is seen that, although the plasma velocity decreases with increasing molecular weight of the gas, the velocities for the gases heavier than hydrogen do not differ by much. Essentially the same results were obtained with a similar accelerator which had a different set of electrodes, capacitor bank, and type of propellant valve.

In interpreting these results, it must be remembered that, since the gas is admitted by a valve and because the gas supply pressures differed, the density of the gas in the interelectrode space at the initiation of the discharge is different for each gas, even though the valve is operated in exactly the same manner. Consequently, the effect of the gas itself cannot be determined from this data. It does appear, however,

that for a pinch accelerator in which the discharge is initiated by the propellant admitted from a valve, the plasma velocity does not differ much for any gas except hydrogen.

These results are similar to those obtained by Michels and Ramins(10) using a coaxial plasma gun. They used hydrogen, nitrogen, and argon and found that the variation of magnetic front velocity was very small when the mass of each gas admitted was approximately the same. They also found that the magnetic front velocity decreased slightly with increasing molecular weight of the gas.

It should be noted that in Ref. 1 the plasma velocity appeared to vary linearly with the energy stored in the capacitors. In Fig. 13 it is seen that the curve for hydrogen deviates from a straight line at about 250 joules and the curves for the heavier gases deviate at somewhat higher energies. However, the deviation for the heavier gases is quite small. The discrepancy between Fig. 13 and the data reported in Ref. 1 can be attributed to the greater scatter of the previous data.

ELECTRON DENSITY

Indications of the electron density in the accelerator exhaust were obtained from microwave interferometer(11) and double electric probe measurements. It was estimated that the maximum electron density is over 10^{14} electrons/cm^3 and may be as high as 5×10^{15}

electrons/cm^3. These estimates are higher than previous estimates of the exhaust electron density (1). Exact measurements could not be made since microwave equipment is not available which will measure densities over 10^{14} electrons/cm^3 and probe theory to date is valid only for lower densities. Work is currently in progress to obtain more accurate measurements.

CONCLUSIONS

The important conclusions resulting from this study can be summarized as follows:

1) The current sheet propagates down the electrodes becoming more diffuse with time. Its minimum thickness is about 4 cm.
2) Only the current sheet, due to the first half-cycle of current, propagates down the electrodes. Therefore, only one pinch is produced.
3) The motion of the current sheet turns from the radial to the axial direction. The magnetic force on the plasma is approximately in the direction of plasma motion.
4) There are regions behind the current sheet where the direction of current shows local reversals.
5) The magnetic impulse represents the largest part of the impulse produced by the accelerator.

6) All of the net energy transferred from the capacitors to the accelerator is transferred during the first 2.4 μsec.

7) The plasma exhaust velocity decreased with increasing molecular weight of the propellant, but the variation with molecular weight was small.

ACKNOWLEDGMENTS

The authors would like to thank W. McIlroy for many stimulating discussions, T. Donner for calibrating the voltage dividers, F. Petri for aiding in the reduction of the experimental data, and the personnel of the experimental laboratory for building and assisting in the operation of the apparatus.

REFERENCES

1 Aronowitz, L. and Duclos, D. P., "Characteristics of the pinch discharge in a pulsed plasma accelerator," Preprint 2367-62. ARS Electrical Propulsion Conference, Berkeley, California, March 14-16, 1962. To be published in Electric Propulsion Development, ARS Progress in Astronautics and Rocketry Series, Vol. 9, 1963.

2 Glasstone, S. and Lovberg, R.H., Controlled Thermonuclear Reactions, (D. Van Nostrand Co. Inc., Princeton, N.J., 1960) p. 230.

3 Sergre, S. E. and Allen, T. E., "Magnetic probes of high frequency response," Jour. Sci. Inst., 37, 369-370 (1960).

4 Gooding, T. J., Hayworth, B. R. and Lovberg, R. H., "Instabilities in a coaxial plasma gun," ARS Preprint 2665-62 (November 1962).

5 Burkhardt, L. C. and Lovberg, R. H., "Current sheet in a coaxial plasma gun," Phys. Fluids, 5, 341-347 (1962).

6 Gloersen, P., "Pulsed plasma accelerators," ARS Preprint 2129-61 (October 1961).

7 Guman, W. J., Personal communication.

8 Hart, P. J., "Plasma acceleration with coaxial electrodes," Phys. Fluids, 5, 38-47 (1962).

9 McIlroy, W. and Siegel, B., "Analysis of factors influencing plasma engine performance," presented at ASME Hydraulics, Gas Turbine, Aviation and Space Meeting, Los Angeles, March 3-7, 1963.

10 Michels, C. J. and Ramins, P., "Performance of coaxial plasma gun with various propellants," presented at the International Symposium on Plasma Coaxial Guns, Cleveland, September 6-7, 1962.

11 Levy, G. and Steinberg, A., "Determination of pinch plasma engine exhaust profiles by microwave interferometry techniques," to be presented at the IRE International Convention, New York, March 25-28, 1963.

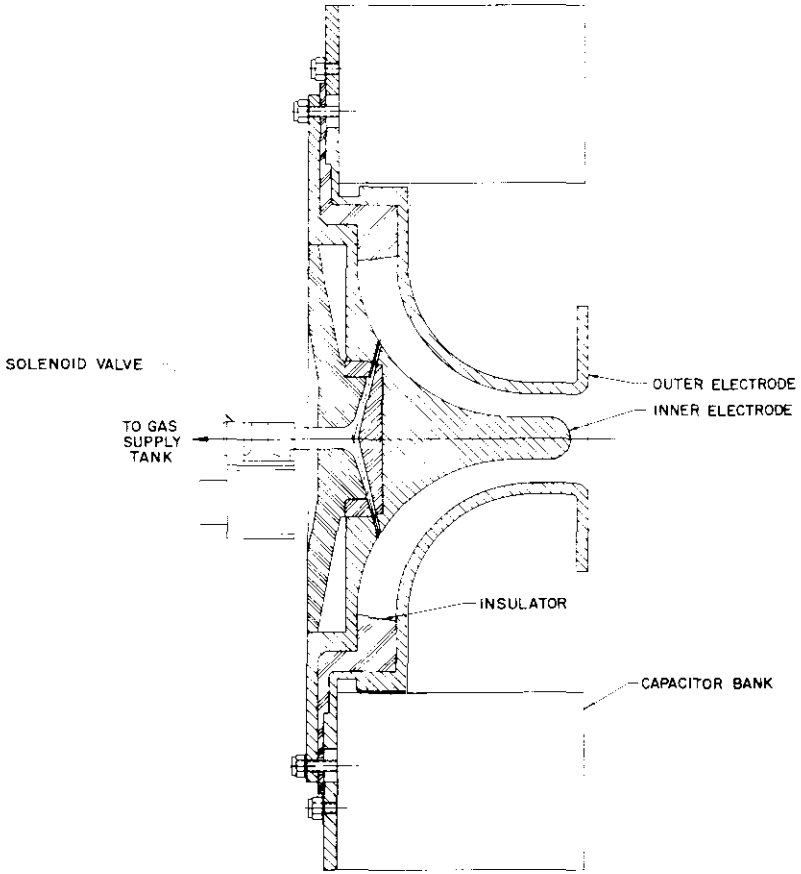

Fig. 1 Schematic of pinch plasma accelerator

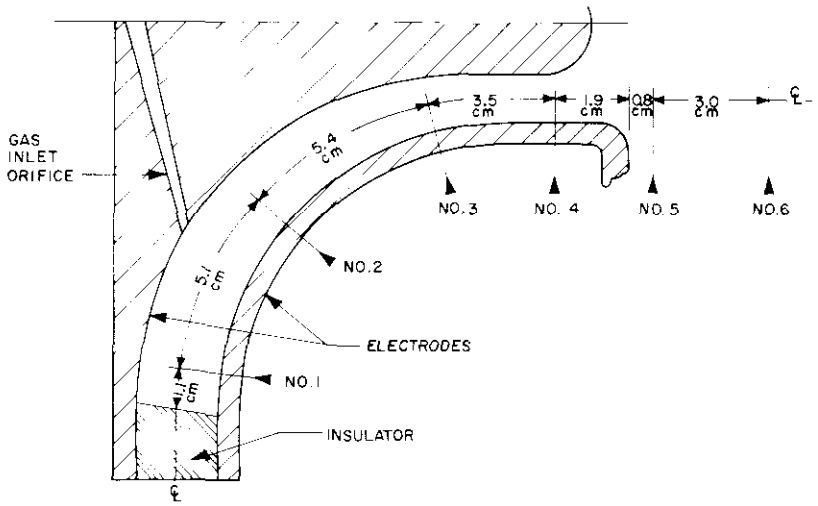

Fig. 2 Accelerator electrodes showing probe positions

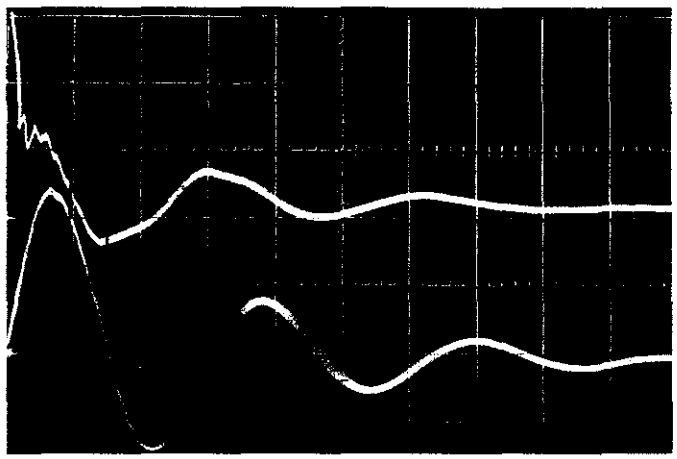

Fig. 3 Typical capacitor voltage and total discharge current traces, initial capacitor voltage = 3 kv, sweep speed = 2 μsec/division. Upper trace: V_c, gain = 1 kv/division (zero voltage is 3 divisions from top). Lower trace: I, gain = 78.4 ka/division

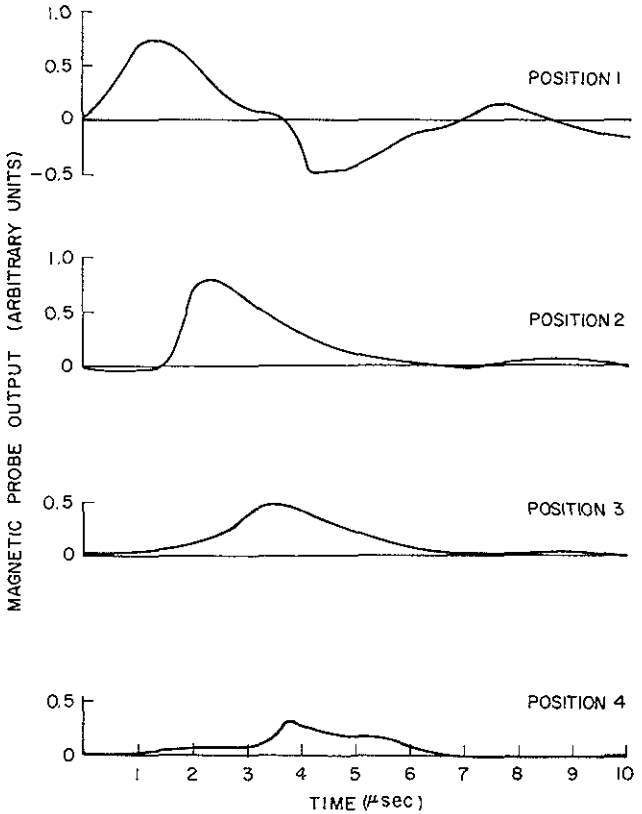

Fig. 4 Magnetic probe output vs. time

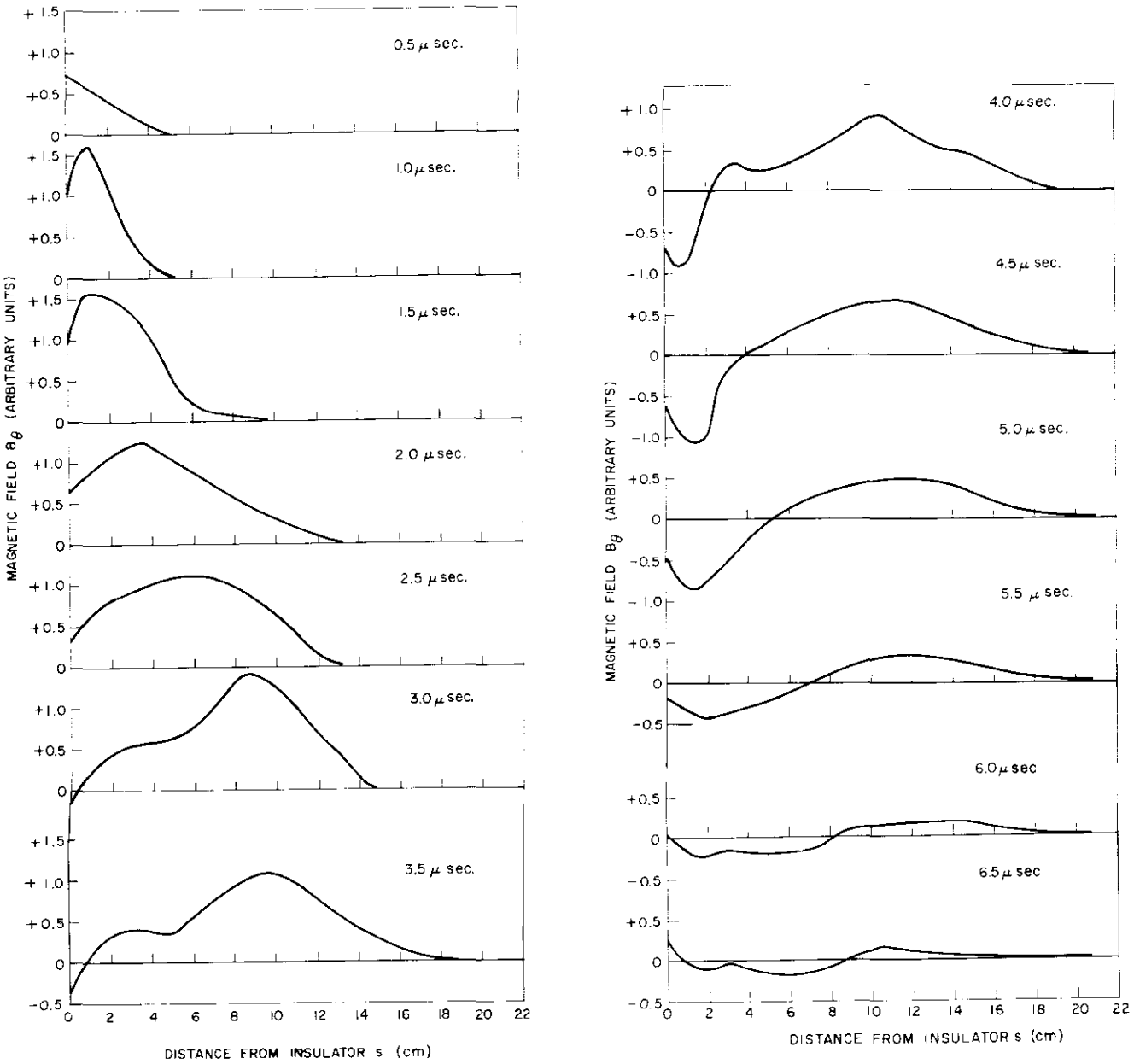

Fig. 5 Magnetic field vs. distance from insulator

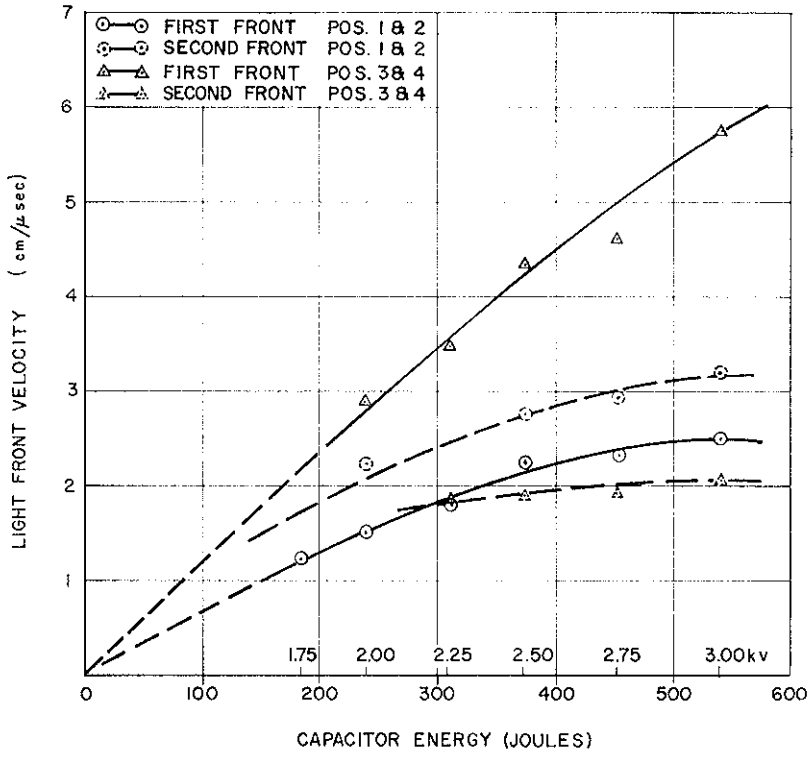

Fig. 6 Velocity of first and second light fronts vs. capacitor energy

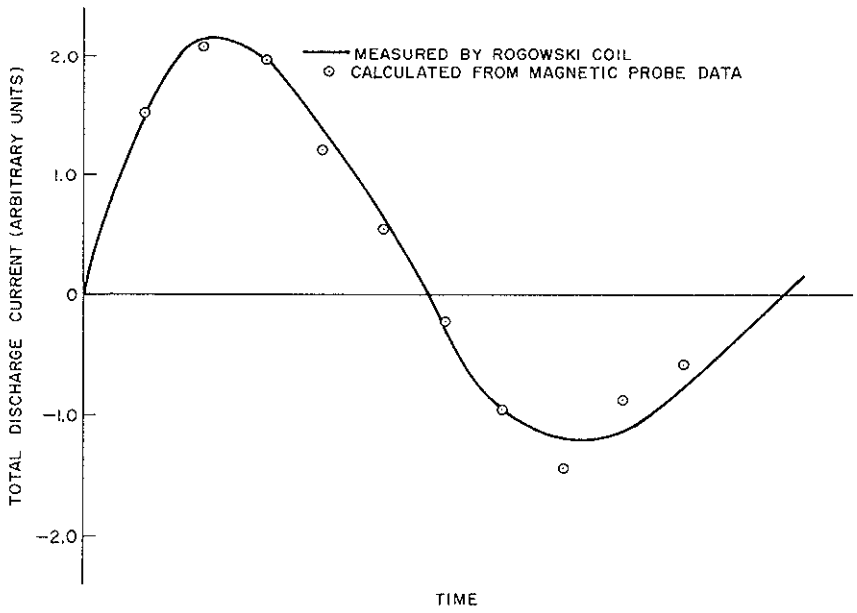

Fig. 7 Comparison of total discharge current measured by Rogowski coil with values calculated from magnetic probe data

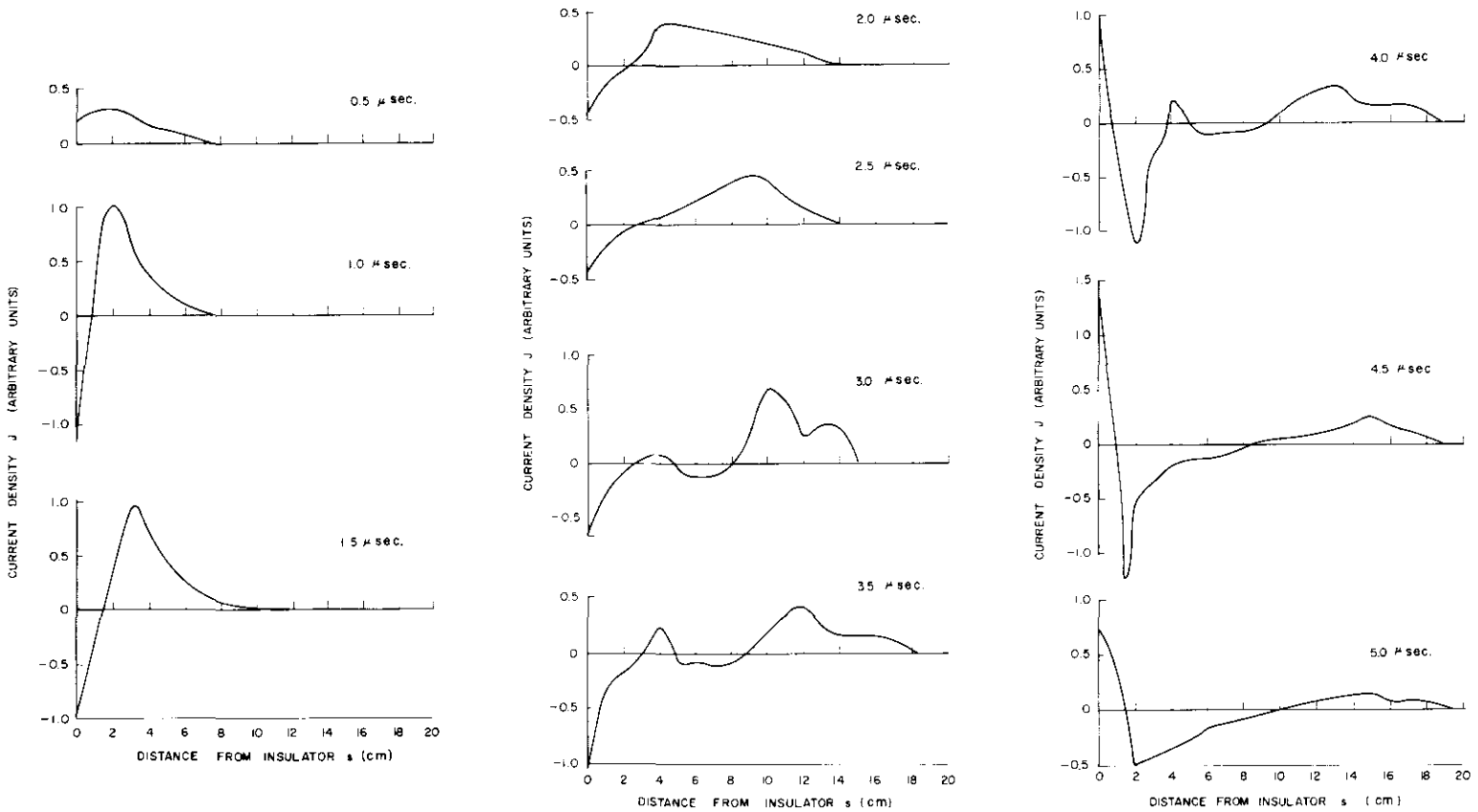

Fig. 8 Current density vs. distance from insulator

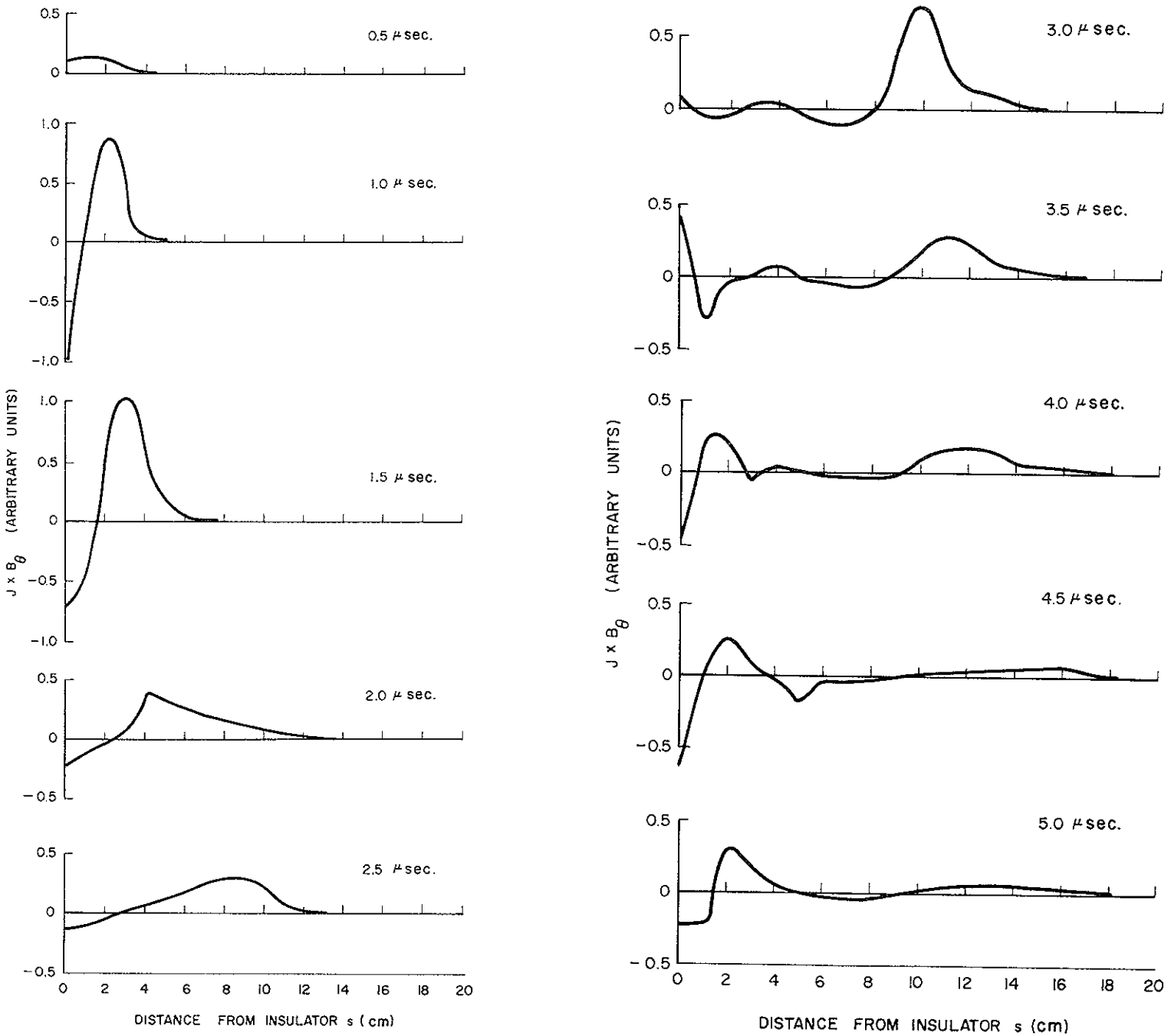

Fig. 9 J x B force vs. distance from insulator

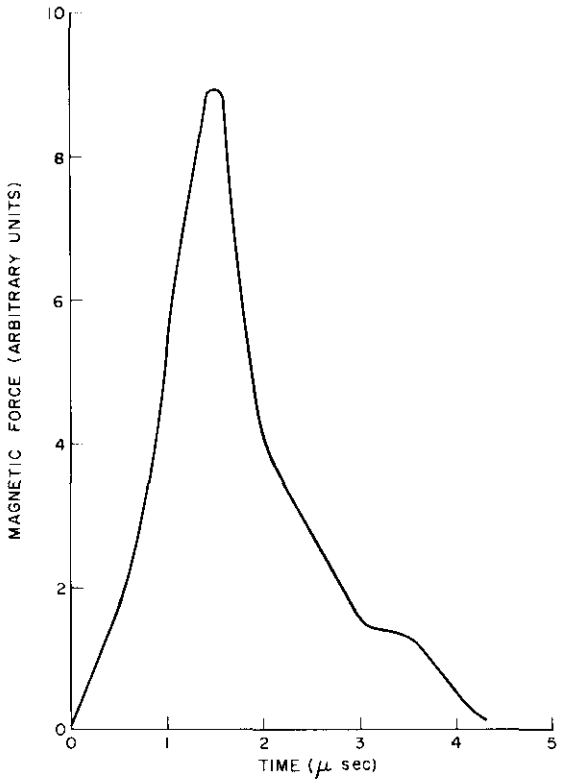

Fig. 10 Magnetic force on plasma vs. time

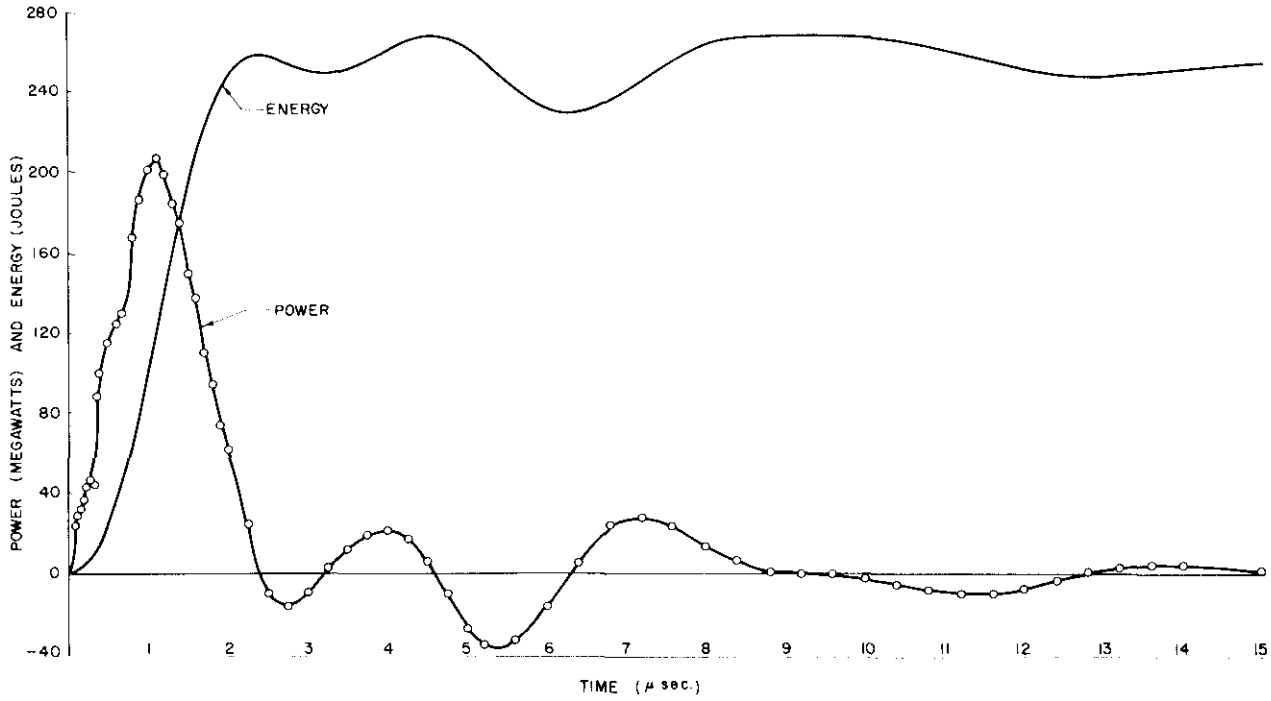

Fig. 11 Power and energy output of capacitor bank vs. time

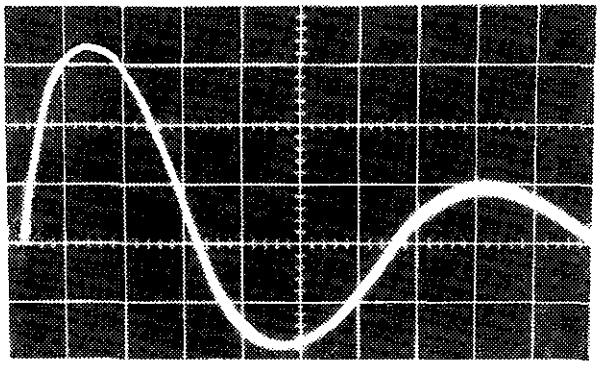

(a) Short circuited electrodes

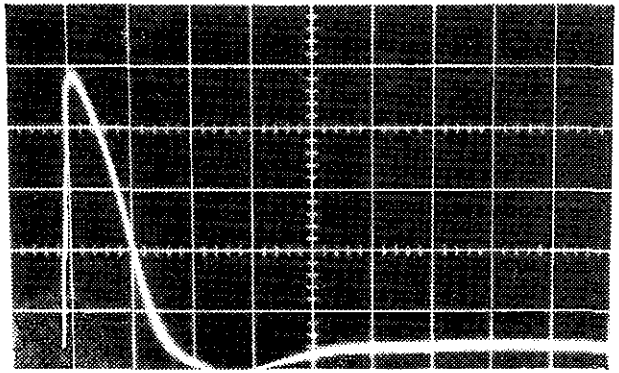

(b) Discharge

Fig. 12 Total current traces of "matched" accelerator

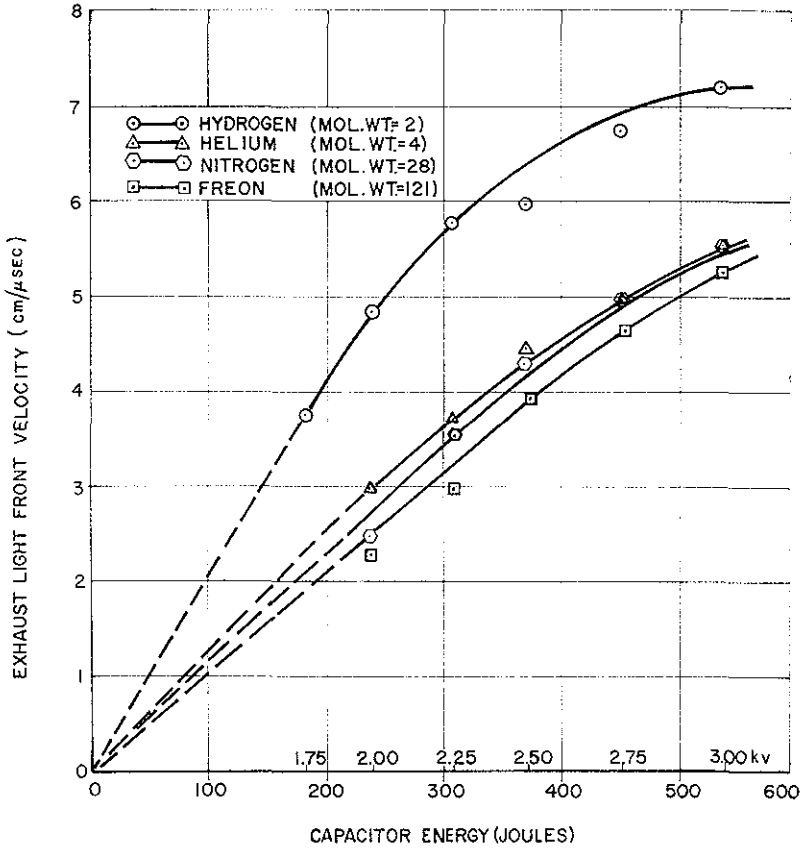

Fig. 13 Light front velocity of exhaust plasma vs. capacitor energy for various propellants